



Structure of Al/Organometallic Complex/p-Si Investigation of Electrical Properties

Hülya Doğan

Sivas Cumhuriyet University, Faculty of Engineering, Department of Electrical- Electronic Engineering, Sivas, Turkey, (ORCID: 0000-0002-5501-2194),
hdogan@cumhuriyet.edu.tr

(First received 31 October 2022 and in final form 17 December 2022)

(DOI: 10.31590/ejosat.1196948)

ATIF/REFERENCE: Doğan, H. (2023). Structure of Al/Organometallic Complex/p-Si Investigation of Electrical Properties. *Avrupa Bilim ve Teknoloji Dergisi*, (46), 64-73.

Abstract

Spin coating was used to deposit the interfacial layer of the organometallic complex (OM complex) as a thin film on p-Si. Al/OM complex/p-Si Schottky diode structure was achieved at room temperature after the required procedures. Current-Voltage (I-V) and Capacitance-Voltage (C-V) measurements of an interface-layered Schottky diode were used to compute the diode's characteristic parameters. Among the I-V readings, the barrier height (Φ_{b0}) and ideality factor (n) were computed, and the results were 0.797 eV and 1.615, respectively. The series resistance (R_s) was found and compared with the Cheung and Norde functions. Additionally, doping density (N_a) values and barrier height were found out from C-V measurements in the frequency range of 10 kHz to 1 MHz, and the Φ_{b0} values from I-V and C-V observations were compared. The difference in the barrier height values obtained from I-V and C-V was attributed to the inhomogeneity of the barrier height, the presence of the interfacial layer, the thickness of the interface layer and the series resistance effect, as well as the different nature of both methods.

Keywords: Organometallic complex, Schottky diode, Barrier height.

Al/Organometalik Kompleks/p-Si Yapısının Elektriksel Özelliklerinin İncelenmesi

Özet

Organometalik kompleksi (OMcomplex) arayüzey tabakası olarak p-Si üzerinde ince bir film olarak biriktirmek için döndürmeli kaplama kullanıldı. Al/OMcomplex/p-Si Schottky diyot yapısı gerekli işlemlerden sonra oda sıcaklığında elde edilmiştir. Arayüz katmanlı Schottky diyotun Akım-Gerilim (I-V) ve Kapasitans-Gerilim (C-V) ölçümleri diyotun karakteristik parametrelerini hesaplamak için kullanıldı. I-V okumalarından bariyer yüksekliği (Φ_{b0}) ve idealite faktörü (n) hesaplandı ve sonuçlar sırasıyla 0.797 eV ve 1.615 oldu. Seri direnç (R_s), Cheung ve Norde fonksiyonları ile bulunarak karşılaştırıldı. Ayrıca 10 kHz ile 1 MHz frekans aralığında yapılan C-V ölçümlerinden doping yoğunluğu (N_a) değerleri ve engel yüksekliği bulunmuş ve I-V ve C-V gözlemlerinden ulaşılan Φ_{b0} değerleri karşılaştırılmıştır. I-V ve C-V den elde edilen engel yüksekliği değerlerinin farklılığı, engel yüksekliğinin homojen olmayışı, arayüzey tabakasının varlığı, arayüzey tabakasının kalınlığı ve seri direnç etkilerinin yanı sıra her iki yöntemin farklı tabiatına atfedilmiştir.

Anahtar Kelimeler: Organometalik kompleks, Schottky diyot, Bariyer yüksekliği.

1. Introduction

A metal/semiconductor (MS) contact can be either ohmic or a rectifier. The rectifier MS contact is called a Schottky barrier diode (SBD) and is a device based on majority carriers [1]. Schottky barrier diodes (SBDs) are basically formed by contacting metal and semiconductor with each other in high temperature, low-pressure environment with the least possible resistance. Electronic and optoelectronic devices like light-emitting diodes, solar cells, field effect transistors, electroluminescent devices, and sensors frequently make use of organic materials [2]. Organic materials are preferred because of their attractive properties such as easy synthesis and ease of processing, environmental stability, compatibility with flexible substrates, and low material consumption for molecular ultrathin films. In addition to these features, they offer the hope of cheaper photovoltaic power generation [3,4]. A thin organic layer placed between a metal-semiconductor (MS) structure and its components can change its electrical properties. According to earlier research, adding an organic thin interlayer between the metal and semiconductor can change the MS diode's barrier height [5-9].

Organometallic complex (OMC) compounds have received increased attention in recent investigations on electrical and optoelectronic devices. Numerous investigations have been made into the properties of ruthenium (II) complexes' thermal stability, photochemistry, photophysics, and electrochemistry [10]. Because it is known that the oxidation states of transition metals can be greatly altered by enhancing the electron transfer processes, research on molecular electronics involving transition metal complexes has generated a lot of interest [11]. The chemistry of organometallic complexes, which are used as valuable interlayers in charge transfer processes in metal-semiconductor (MS) diodes, is very important [12]. These characteristics have influenced the creation of various ruthenium (II) complex applications (e.g. artificial photosynthetic frameworks [13], sensors [14], and catalysis [15]). Dye-sensitized solar cells (DSCs) have garnered a lot of interest among these applications as a potential substitute for conventional silicon photovoltaic systems [16,17]. In particular, O'Regan and Gratzel [18] developed a dye-sensitized solar cell that uses a Ru (II) complex that is low cost and high in efficiency. Phthalocyanine complexes have been used to create several Schottky diodes and solar cells [19,20]. Schottky diode generation by a newly created, synthetic Mn hexamine (MnHA) organometallic complex (OMC) has been demonstrated by Ocak et al. [21]. Therefore, there is considerable interest in both the development of new organometallic compounds and the use of those compounds in the manufacture of devices.

Metal complexes are used in electronic applications due to their essential electrical and optical characteristics. Ru (II) complexes are crucial components because of their electronic, optical, and chemical characteristics. Using the drop-casting method, Tataroglu et al. [22] investigated the creation of an Au/Ruthenium (II) complex/n-Si photodiode. They [22] analyzed the electrical and photo response properties of Photodiode-based Ruthenium (II) complex dye with capacitance and conductivity measurements over a wide range of luminous intensity and frequency. By using the spin coating approach, Soyulu et al. [23] created a Ruthenium (II) complex with polydentate pyridine on the surface of a Si substrate. They [23] used illumination-dependent I-V measurements to demonstrate these photovoltaic characteristics. Doğan et al. [24] coated tris (2,2'-bipyridine) Ruthenium (II)-a complex by spin coating method as a thin layer on p-type crystalline silicon by rotating at 500 rpm for one minute in order to form Al/Ru(II)/p-Si photodiode. They [24] calculated the solar cell characteristics of this structure and also calculated the Schottky barrier height, ideality factor and series resistance value from the I-V characteristics in a dark environment.

In this study, Al/OM complex/p-Si diodes were formed using organometallic complex. Because it is a substance rich in π -bonds, the OM complex molecule with the closed formula (C₃₀H₂₄F₁₂N₆P₂Ru) (see figure 1) was selected as the interfacial layer in the metal/semiconductor structure. Certain diode parameters were obtained and compared by using capacitance-voltage (C-V), electrical current-voltage (I-V), and reverse bias C⁻²-V characteristics at room temperature.

2. Material and Method

2.1. Experimental Details

The p-type silicon semiconductor used in this study has a thickness of 525 nm, an orientation of (100), and a specific resistance that ranges from 1 to 10 cm. Chemical cleaning of the p-Si wafer was done using the RCA cleaning method [25]. After cleaning, a 100 nm layer of aluminium metal was produced using the thermal evaporation (deposition) method on the matter surface in preparation for the ohmic contact procedure. The sample was annealed for three minutes in an oven that had been warmed to 450 C under nitrogen gas to complete the ohmic contact treatment. Following the ohmic contact approach, a tris (2,2'- bipyridine) ruthenium (II) organometallic complex from Sigma Aldrich was used as an intermediary layer. Ethanol was used to create a Ru (II) (0.01 M) solution for this technique. the p-Si substrate's front surface was covered with 5 mL of an alcohol-based 0.001 M Ru (II) solution. After being spun onto the Si substrate for 30 seconds at 2000 revolutions per minute, to remove the solvent, the solution was then dried for 60 minutes at room temperature. A mask with a diameter of 1 mm was applied to the Ru (II) complex after it had formed, and aluminium metal was formed with a thickness of 100 nm by the thermal evaporation method. As a result, the Al/OM complex/p-Si/Al structure (figure 1) was obtained. All evaporation procedures were accomplished at 4×10^{-6} Torr pressure and under vacuum. The samples were measured for current-voltage (I-V) and capacitance-voltage (C-V) using a Keithley 4200 SCS.

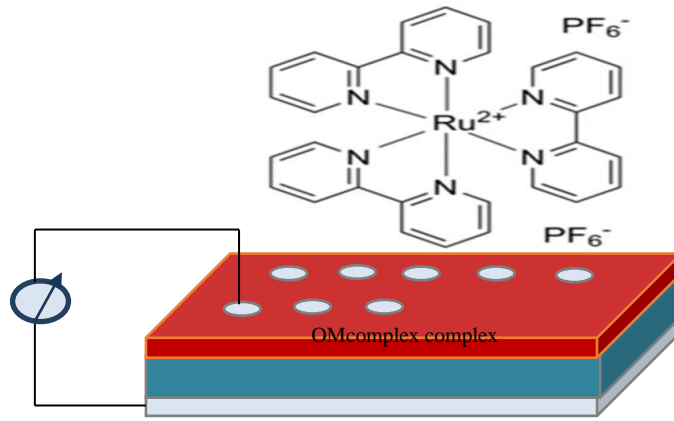


Figure 1. Chemical structure of the organometallic (OM) complex and device structure of Al/OM complex/p-Si/Al [24].

3. Results and Discussion

To determine the diode features of the Al/OMcomplex/p-Si diode, forward and reverse I-V measurements were taken in the ± 2 V range and their graphs are shown in Figure 2 (a) and (b). As can be observed from the sample's I-V characteristic, there is a potential barrier at the interface, and it exhibits a rectifying property [26]. Due to the diode's series resistance to the high values of the applied voltage, a bend has occurred in the graph. This limited the diode current (Fig. 2a).

Thermionic emission theory claims that the relationship between the current flowing through a Schottky barrier and the voltage applied to the contact is also taken into account by the series resistance (R_s) effect. Given as (1):

$$I = I_0 \left[\exp \left(\frac{q(V - IR_s)}{nkT} \right) - 1 \right] \quad (1)$$

The ideality factor here is "n" and its value is unity for an ideal diode. For $V > 3kT/q$, the value of 1 in parentheses can be neglected in the equation. In the expression the Boltzmann constant is k, T is the ambient temperature in Kelvin, and I_0 is the extrapolated saturation current value.

Here, I_0 is given as follows.

$$I_0 = AA^*T^2 \exp \left(-\frac{q\Phi_{b0}}{kT} \right) \quad (2)$$

q represents the electronic charge ($=1,6 \times 10^{-19} \text{C}$), V is for the applied voltage, A represents the effective diode area ($=7,85 \times 10^{-3} \text{cm}^2$), Φ_{b0} is the apparent barrier height with zero bias (BH), A^* is the p-type silicon's effective Richardson constant, which is $32 \text{ A cm}^{-2} \text{ K}^{-2}$. Equation (1) is used to determine the diodes' ideality factors. You can get the following expression by using (1).

$$n = \frac{q}{kT} \frac{dV}{d(\ln I)} \quad (3)$$

In this expression, the value of the term $dV/d(\ln I)$ is obtained from the slope of the linear part on the right-feed side of the $\ln I$ -V graph (Fig. 2b). If Equation 2 is rearranged, the following expression is obtained for the zero-bias barrier height.

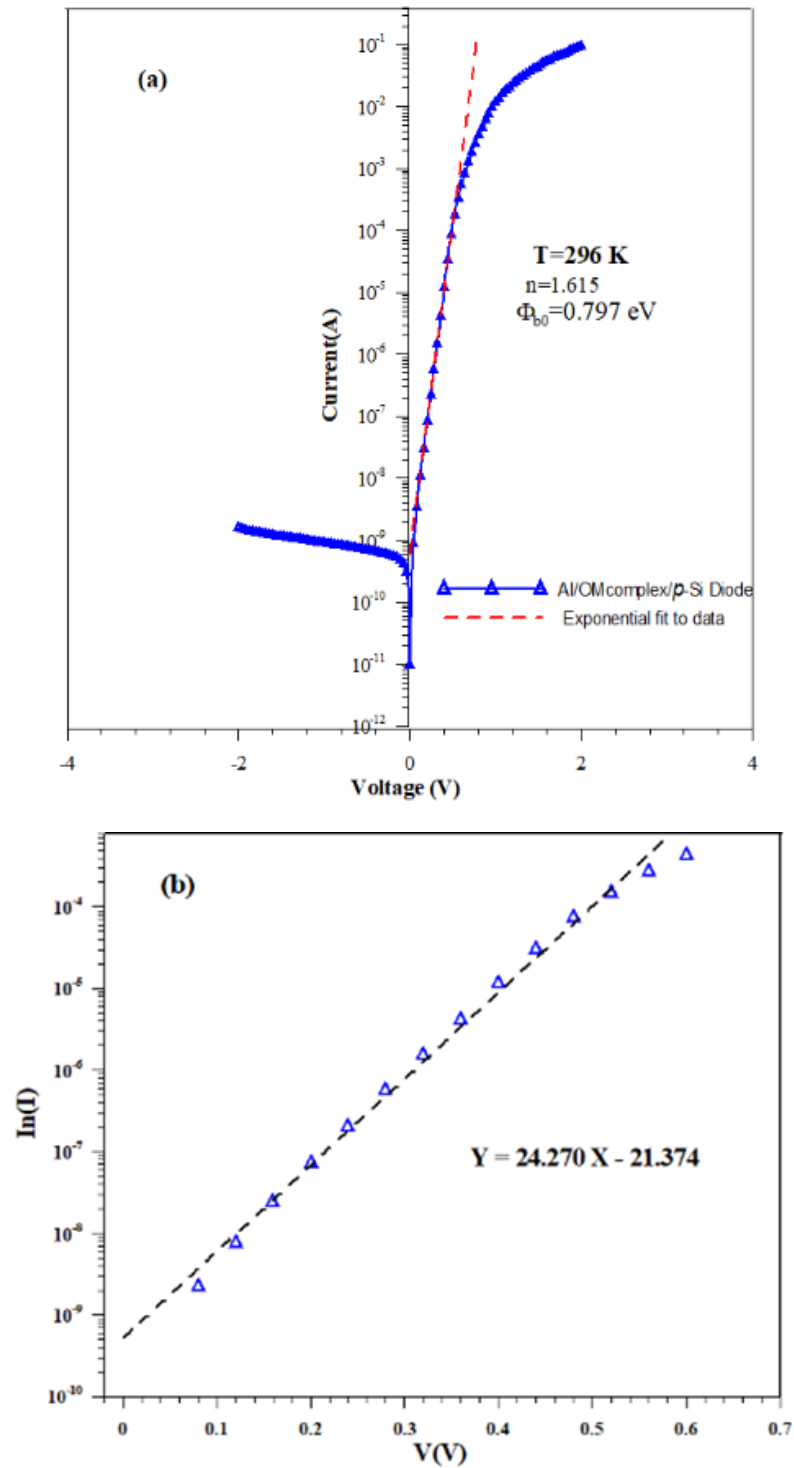


Figure 2. (a): Forward and reverse bias I – V plots of the Al/OMcomplex/p-Si Schottky contacts at 296 K. **(b)** ln (I)-V characteristic of Al/OMcomplex/p-Si Schottky diode in the range of 0.04V-0.60V

$$q\Phi_{b0} = kT \ln \left(\frac{AA^*T^2}{I_0} \right) \quad (4)$$

A linear fit has been applied to the $\ln I$ - V graph, as seen in Figure 2b, using the so-called traditional I-V method. With the help of equations (2), (3) and (4), diode parameters n , Φ_{b0} and I_0 are obtained. These parameters are found as 1.615, 0.797 eV and 6.008×10^{-10} A respectively. The existence of barrier inhomogeneities, interfacial states between metal and semiconductor, and series resistance can be used to explain why this is the case [27-28].

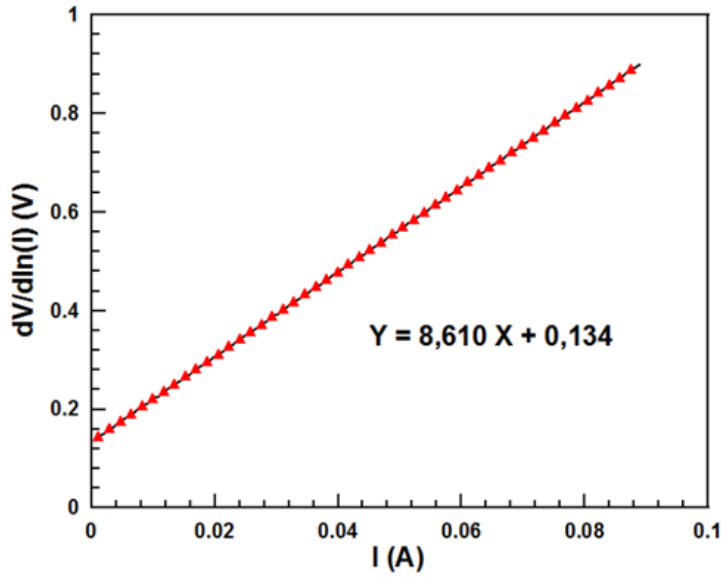


Figure 3. Experimental $dV/d\ln(I)$ vs. I plots of Al/OMcomplex/ p -Si at room temperature

The series resistance effect is one of the factors that contribute to the ideality factor being greater than 1. The series resistance effect is what causes the forward bias current-voltage curves to bend at high voltages. Equations (5) and (6) are called Cheung functions in the literature [29]. In accordance with Eq. 5, the slopes of the $dV/d(\ln I)$ - I plot were used to determine the values of R_s . As seen in Figure 3, the value of R_s was found to be 8,610 ohms and the ideality factor (n) to be 5,248.

$$\frac{dV}{d(\ln I)} = \frac{nkT}{q} + IR_s \quad (5)$$

$$H(I) = V - \frac{nkT}{q} \ln\left(\frac{I}{AA^*T^2}\right) \quad (6a)$$

$$H(I) = n\Phi_b + IR_s \quad (6b)$$

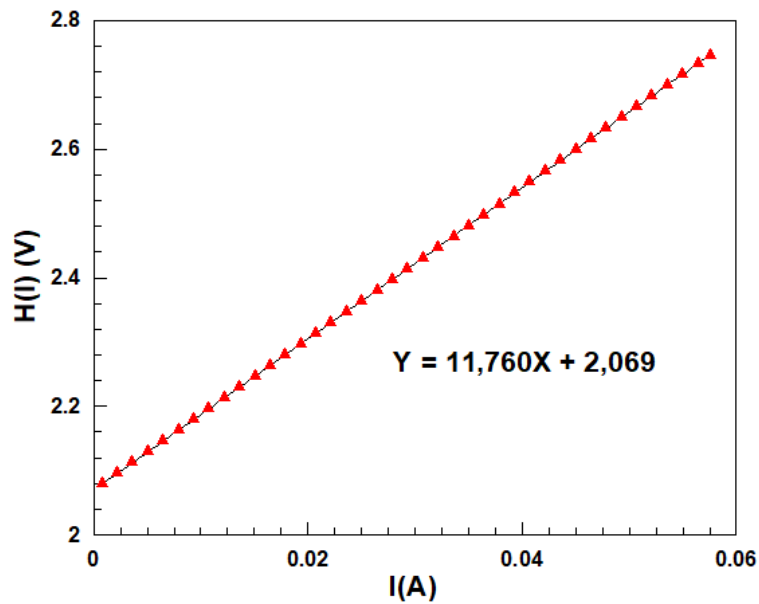


Figure 4. Experimental $H(I)$ vs. I plots of Al/OMcomplex/ p -Si at room temperature.

Considering the Cheung function in Equation (6a), the $H(I)$ - I graph of the diode is drawn. A linear fit was applied to the $H(I)$ - I graph in Figure 4 and Φ_b and R_s values were obtained with the help of Equation (6b). The barrier height value was calculated as 0.394 eV and the series resistance value was calculated as 11,760 ohm (see Table 1).

The ideality factor is more than one due to the Organometallic complex (Ru(II)) at the interface and the natural thin oxide layer on the p-Si. The presence of the OM complex as an interfacial layer changes the characteristic parameters of organic-inorganic structures, since it affects the series resistivity and bulk resistivity.

The Norde [30] approach is another technique used to figure out the Schottky diode's series resistance. The Norde method is not suitable for finding contact parameters in non-ideal ($n > 1$) situations, as it assumes that the contact between metal and semiconductor is ideal. For this reason, Bohlin [31] modified this method for non-ideal cases. Bohlin's generalized method makes it possible to calculate Φ_b and R_s values from a single I-V measurement taken at a constant temperature. This method defines the modified Norde function as follows.

$$F(V; \alpha) = \frac{V}{\alpha} - \frac{kT}{q} \ln \left(\frac{I(V)}{AA^*T^2} \right) \quad (7)$$

Here α is an arbitrary constant greater than the ideality factor. The Schottky diode parameters barrier height (Φ_b) and series resistance (R_s) are provided in equations 8 and 9, respectively, using the Norde function.

$$\Phi_b = F_{min}(V, \alpha) + \left(\frac{\alpha-n}{n} \right) \left(\frac{V_{min}}{\alpha} - \frac{kT}{q} \right) \quad (8)$$

$$R_s = \frac{kT(\alpha-n)}{qI_{min}} \quad (9)$$

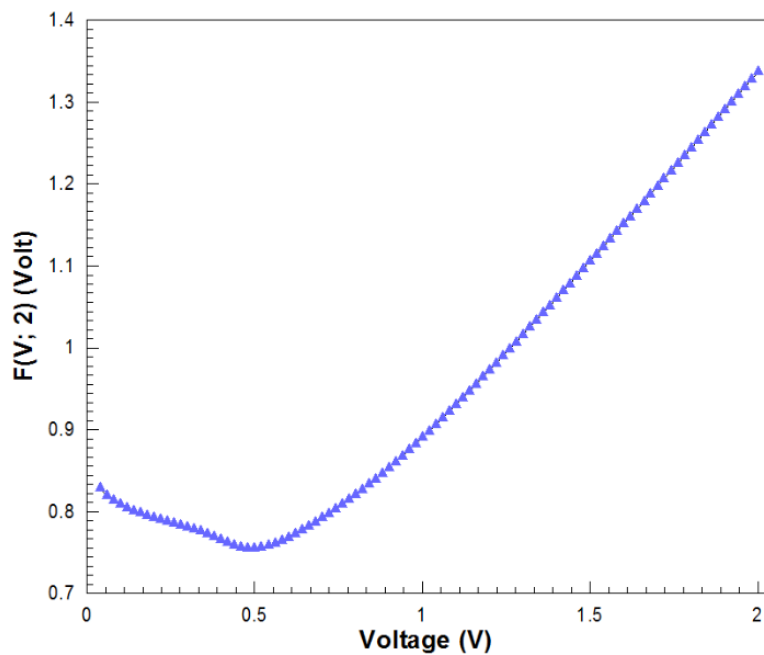


Figure 5. $F(V;2)$ - V curve obtained from I-V data of Al/OMcomplex/p-Si Schottky diode at room temperature.

Φ_b parameters, the $n=1.615$ value obtained from the traditional method was used. As seen in Table 1, the $R_s=78,003\Omega$ value obtained from this method is different from that obtained from the Cheung functions. Plots of auxiliary functions are used in Norde and Cheung's approach to evaluate the diode parameters more precisely. Despite this, the techniques also have flaws of their own. The n is thought to be quite close to unity in Norde's functions. For a real Schottky contact, this is not typically the case.

Table 1. Comparison of diode parameters obtained from different methods

Method		n	Φ_b (eV)	R_s (Ω)
Traditional	<i>I-V</i>	1,615	0,797	
Cheung	<i>dV/dlnI-I</i>	5,248		8,610
	<i>H(I)-I</i>		0,397	11,760
Norde	<i>F(V)-V</i>		0,850	78,003

Only a single point of Norde's function graph is used to calculate Φ_b . These are Norde's functions' main problems. As may be observed from the R_s values, we determined using both approaches above, these problems often result in an overestimation of the series resistor value compared to the values determined by the Cheung method (see Table 1).

In Figure 6, the capacitance-voltage (*C-V*) characteristic of the Al/OM complex /*p*-Si Schottky diode is drawn. There is a peak in the *C-V* features. With rising frequency, capacitance's peak value falls. As the frequency decreases, the capacitance begins to increase. It is a sign that the distribution of interface states is continuous. At low frequencies, the capacitance is equal to the product of the interface capacitance and the space charge capacitance, however at higher frequencies, the space charge capacitance accounts for the majority of the total capacitance [32-35]. At low frequencies, interface states are capable of following the AC signal. High frequencies, though, are impossible for it to follow ($f \geq 1$ MHz).

The *C-V* measuring method is another technique for calculating the barrier height. Figure 7 displays the C^{-2} -*V* graphs of the Al/OM complex/*p*-Si structure at 500 kHz, room temperature, and in the dark. A metal/space semiconductor's charge region's capacitance contains crucial details on the creation of the interface. Calculations of the carrier concentration in the semiconductor, the Fermi energy level, the diffusion potential, and the barrier height of the rectifier contact may all be made using capacitance measurements based on reverse bias voltage [36].

$$\frac{1}{C^2} = \frac{2(V_d + V)}{A^2 \epsilon_s \epsilon_0 e N_a} \quad (10)$$

ϵ_s denotes the semiconductor dielectric constant (for Si, $\epsilon_s=11.8$), ϵ_0 define the vacuum permittivity (8.85×10^{-14} F/cm), e denotes the electronic charge (1.6×10^{-19} C), V_0 denotes the diffusion potential, k denotes the Boltzmann constant, N_a denotes the concentration of ionized acceptors, T define the ambient temperature in Kelvin (K), and A denote the effective area of the diode.

The barrier height can be determined using the relationship shown below.

$$\Phi_{b0} = \frac{V_d}{n} + V_p \quad (11)$$

Here, V_p is the difference between the top of the valence band and the fermi level of the neutral part of *p*-type Silicon and is expressed as follows:

$$V_p = \frac{kT}{e} \ln \frac{N_v}{N_a} \quad (12)$$

Here, N_v is used to represent the effective density of silicon's valence band, and $1.04 \times 10^{-4} \text{ cm}^{-3}$ is used as the value.

According to Equation (10), when $C^{-2}=0$ in the C^{-2} -*V* graph, the diffusion potential was determined with the help of the V_0 shear potential, which is the point where the horizontal axis (voltage axis) and the line cross. Therefore, it is found as diffusion potential ($V_d=0.481$ V). The barrier height was found ($\Phi_{b0}=0.816$ eV) using Equations (11) and (12). In the dark, the barrier height determined by *C-V* measurements is greater than the barrier height determined by *I-V* observations ($\Phi_{b0}=0.81$ eV).

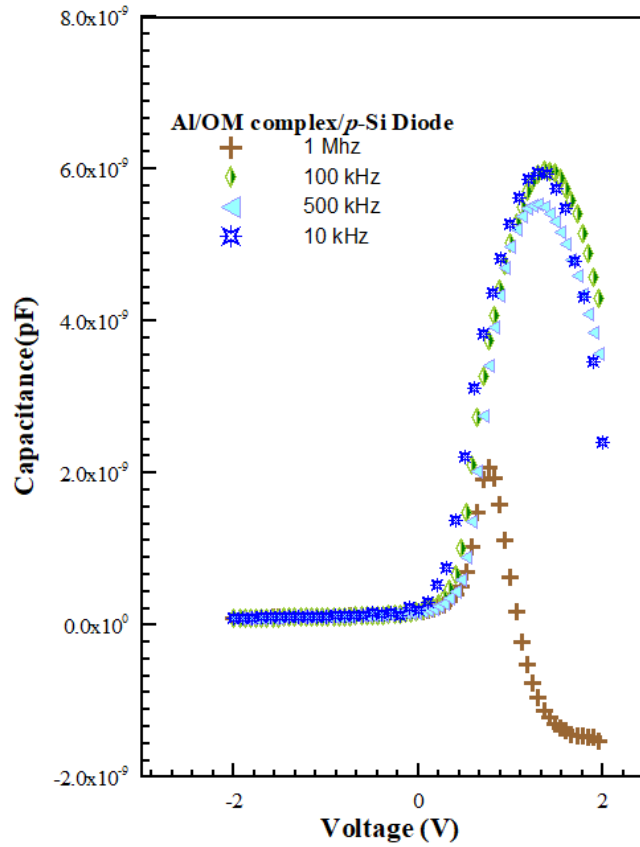


Figure 6. C-V curves of Al/OMcomplex/p-Si Schottky diode at different frequencies at room temperature.

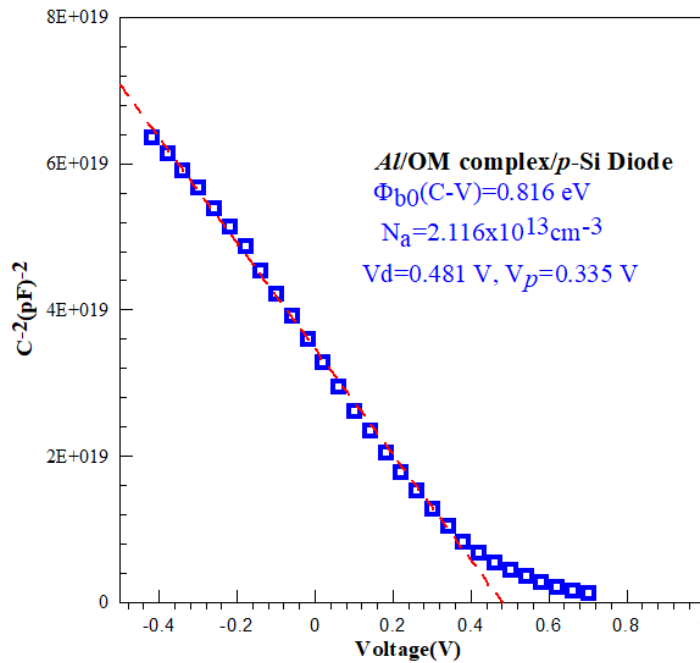


Figure 7. C^{-2} -V characteristic of Al/OM complex/p-Si diode at 500 kHz frequency.

Because of the barrier inhomogeneities in the interfacial layer thickness and interfacial charge distributions, the $\Phi_{b0}(C-V)$ value generated is larger than the $\Phi_{b0}(I-V)$ value. In previous studies on Ru (II) complex/p-Si, barrier heights were reported as 0.84eV [24].

4. Conclusion

By using the spin coating method and thermal evaporation, an Al/OMcomplex/p-Si Schottky diode is created. *I-V* and *C-V* measurements were made for the electrical characterisation of this structure in the dark and at room temperature. Cheung functions were also utilized to determine the barrier height and ideality factor values, which were determined from the *I-V* characteristics, to control their consistency. The ideality factor and barrier height were calculated using the appropriate feeding *I-V* characteristics, and they were determined to be 1.61 and 0.797 eV, respectively. From the Cheung functions, the ideality value was determined as 5.248; R_s as 8,610 ohms and 11,760 ohms; barrier height value as 0.397 eV. The value of $R_s=78.003$ ohms obtained from the Norde method was considerably larger than that obtained from the Cheung functions. It was discovered that 0.850 eV was the barrier height value determined by the Norde method. Additionally, it was seen that the diode capacitance reduced as the frequency increased when the *C-V* characteristics were looked at because the interface states were unable to follow the AC signal. The barrier height of 0.816 eV was determined using the *C²-V* characteristics at 500 kHz. Among these characteristics, the diffusion potential was determined as 0.481 V, the receiver density as $2.116 \times 10^{13} \text{ cm}^{-3}$, and the Fermi energy level as 0.335 V.

References

- [1] Türüt, A. (2020). On current-voltage and capacitance-voltage characteristics of metal-semiconductor contacts. *Turkish Journal of Physics*, 44(4), 302-347.
- [2] Shirota, Y. (2000). Organic materials for electronic and optoelectronic devices Basis of a presentation given at Materials Chemistry Discussion No. 2, 13–15 September 1999, University of Nottingham, UK. *Journal of Materials Chemistry*, 10(1), 1-25.
- [3] Gupta, R. K., Ghosh, K., & Kahol, P. K. (2009). Fabrication and electrical characterization of Schottky diode based on 2-amino-4, 5-imidazoledicarbonitrile (AIDCN). *Physica E: Low-Dimensional Systems and Nanostructures*, 41(10), 1832-1834.
- [4] Rajesh, K. R., & Menon, C. S. (2007). Study on the device characteristics of FePc and FePcCl organic thin film Schottky diodes: Influence of oxygen and post deposition annealing. *Journal of non-crystalline solids*, 353(4), 398-404.
- [5] Güllü, Ö., & Türüt, A. (2008). Photovoltaic and electronic properties of quercetin/p-InP solar cells. *Solar Energy materials and Solar cells*, 92(10), 1205-1210.
- [6] Temirci, C., Gülcan, M., Goksen, K., & Sönmez, M. (2011). Metal/semiconductor contact properties of Al/Co (II) complex compounds. *Microelectronic engineering*, 88(1), 41-45.
- [7] Gunduz, B., Yahia, I. S., & Yakuphanoglu, F. (2012). Electrical and photoconductivity properties of p-Si/P3HT/Al and p-Si/P3HT: MEH-PPV/Al organic devices: Comparison study. *Microelectronic Engineering*, 98, 41-57.
- [8] Antohe, S., Tomozeiu, N., & Gogonea, S. (1991). Properties of the Organic-on-Inorganic Semiconductor Barrier Contact Diodes In/PTCDI/p-Si and Ag/CuPc/p-Si. *physica status solidi (a)*, 125(1), 397-408.
- [9] Rajesh, K. R., & Menon, C. S. (2007). Study on the device characteristics of FePc and FePcCl organic thin film Schottky diodes: Influence of oxygen and post deposition annealing. *Journal of non-crystalline solids*, 353(4), 398-404.
- [10] Ashford, D. L., Brennaman, M. K., Brown, R. J., Keinan, S., Concepcion, J. J., Papanikolas, J. M., ... & Meyer, T. J. (2015). Varying the electronic structure of surface-bound ruthenium (II) polypyridyl complexes. *Inorganic Chemistry*, 54(2), 460-469.
- [11] Ilhan, S. (2008). Preparation and characterization of binuclear CuII complexes derived from diamines and dialdehydes. *Journal of Coordination Chemistry*, 61(18), 2884-2895.
- [12] Sánchez-Vergara, M. E., González-Aranzábal, S. A., Saucedo-Arriaga, M. A., Ortiz, A., Alvarez, J. R., & García-Montalvo, V. (2010). Electrical and optical properties of (PPh₄)₂ [Fe (CN) 5NO] non-crystalline thin films prepared with the vacuum thermal evaporation technique. *Journal of non-crystalline solids*, 356(4-5), 244-249.
- [13] MK, C., & Iha, H., (2009). NY Templeton JL Meyer TJ Acc. *Chem. Res*, 42, 1954-1965.
- [14] Beer, P. D., & Cadman, J. (2000). Electrochemical and optical sensing of anions by transition metal based receptors. *Coordination Chemistry Reviews*, 205(1), 131-155.
- [15] Argazzi, R., Iha, N. Y. M., Zabri, H., Odobel, F., & Bignozzi, C. A. (2004). Design of molecular dyes for application in photoelectrochemical and electrochromic devices based on nanocrystalline metal oxide semiconductors. *Coordination Chemistry Reviews*, 248(13-14), 1299-1316.
- [16] Kapilashrami, M., Zhang, Y., Liu, Y. S., Hagfeldt, A., & Guo, J. (2014). Probing the optical property and electronic structure of TiO₂ nanomaterials for renewable energy applications. *Chemical reviews*, 114(19), 9662-9707.
- [17] Fakhruddin, A., Jose, R., Brown, T. M., Fabregat-Santiago, F., & Bisquert, J. (2014). A perspective on the production of dye-sensitized solar modules. *Energy & Environmental Science*, 7(12), 3952-3981. [18] B. O'Regan, M. Gratzel, Nature 353 (1991) 737.
- [19] R.Koeppel, N.S.Sariciftci, P.A.Troshin, R.N.L.Yubovskaya, Applied Physics Letters 87 (2005) 244102.
- [20] Yakuphanoglu, F. (2007). Electronic and photovoltaic properties of Al/p-Si/copper phthalocyanine photodiode junction barrier. *Solar energy materials and solar cells*, 91(13), 1182-1186.
- [21] Ocak, Y. S., Ebeoğlu, M. A., Topal, G., & Kılıçog, T. (2010). Temperature dependent electrical characteristics of an organic-inorganic heterojunction obtained from a novel organometal Mn complex. *Physica B: Condensed Matter*, 405(9), 2329-2333.
- [22] Tataroğlu, A. D. E. M., Dayan, O., Özdemir, N., Serbetci, Z., Al-Ghamdi, A. A., Dere, A., ... & Yakuphanoglu, F. (2016). Single crystal ruthenium (II) complex dye based photodiode. *Dyes and Pigments*, 132, 64-71.
- [23] Soylu, M., Orak, I., Dayan, O., & Serbetci, Z. (2015). A novel photodiode based on Ruthenium (II) complex containing polydentate pyridine as photocatalyst. *Microelectronics Reliability*, 55(12), 2685-2688. Mol. Cryst. Liq. Cryst. Sci. Technol. Sect. A, 380 (2002), p. 45

- [24] Doğan, H., İkrım, O., & Yıldırım, N. (2017). Photovoltaic and Electrical Properties of Al/Ruthenium (II)-complex/p-Si Photodiode. *Cumhuriyet Üniversitesi Fen Edebiyat Fakültesi Fen Bilimleri Dergisi*, 38(2), 329-341.
- [25] Kern, W. (2018). Overview and evolution of silicon wafer cleaning technology. In *Handbook of silicon wafer cleaning technology* (pp. 3-85). William Andrew Publishing.
- [26] Tatarođlu, A. (2013). Comparative study of the electrical properties of Au/n-Si (MS) and Au/Si₃N₄/n-Si (MIS) Schottky diodes. *Chinese Physics B*, 22(6), 068402.
- [27] Wu, X., Schmidt, M. T., & Yang, E. S. (1989). Control of the Schottky barrier using an ultrathin interface metal layer. *Applied physics letters*, 54(3), 268-270.
- [28] Nicollian, E. H. (1982). JR Brews in MOS Physics and Technology.
- [29] Cheung, S. K., & Cheung, N. W. (1986). Extraction of Schottky diode parameters from forward current-voltage characteristics. *Applied physics letters*, 49(2), 85-87.
- [30] Norde, H. (1979). A modified forward I-V plot for Schottky diodes with high series resistance. *Journal of applied physics*, 50(7), 5052-5053.
- [31] Bohlin, K. E. (1986). Generalized Norde plot including determination of the ideality factor. *Journal of Applied Physics*, 60(3), 1223-1224.
- [32] Güçlü, Ç. Ş., Özdemir, A. F., & Aldemir, D. A. (2019). Mo/n-Si Schottky Diyotların Akım-Voltaj ve Kapasite-Voltaj Karakteristiklerinin Analizi. *Düzce Üniversitesi Bilim ve Teknoloji Dergisi*, 7(3), 2142-2155.
- [33] A. Chelkowski, *Dielectric Physics*, Elsevier, Amsterdam, 1980, pp. 97-105.
- [34] Ho, P. S., Yang, E. S., Evans, H. L., & Wu, X. (1986). Electronic states at silicide-silicon interfaces. *Physical review letters*, 56(2), 177..
- [35] Wu, X., Schmidt, M. T., & Yang, E. S. (1989). Control of the Schottky barrier using an ultrathin interface metal layer. *Applied physics letters*, 54(3), 268-270.
- [36] Wilmsen, C. W., 1985. *Physics and Chemistry of III-V Compound Semiconductor Interfaces*. Plenum Press, New York